

Solar Thermal Collector System Modeling and Testing for Novel Solar Cooker

by

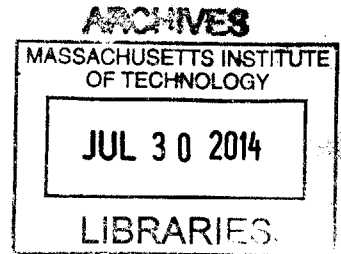
Brian Foley

*Submitted to the
Department of Mechanical Engineering
in Partial Fulfillment of the Requirements for the Degree of
Bachelor of Science in Mechanical Engineering*

at the

Massachusetts Institute of Technology

June 2014



© 2014 Massachusetts Institute of Technology. All rights reserved.

Signature of Author: Signature redacted
Department of Mechanical Engineering
May 23, 2014

Certified by: Signature redacted
David Gordon Wilson
Professor Emeritus of Mechanical Engineering
Thesis Supervisor

Signature redacted
Accepted by: _____
Anette Hosoi
Professor of Mechanical Engineering
Undergraduate Officer

Solar Thermal Collector System Modeling and Testing for Novel Solar Cooker

by

Brian Foley

*Submitted to the Department of Mechanical Engineering
on May 23, 2014 in Partial Fulfillment of the
Requirements for the Degree of
Bachelor of Science in Mechanical Engineering*

ABSTRACT

Solar cookers are aimed at reducing pollution and desertification in the developing world. However, they are often disregarded as they do not give users the ability to cook after daylight hours. The Wilson solar cooker is a solar cooker designed to address this problem by converting solar energy and storing that energy as heat in the form of molten salt (lithium nitrate).

This thesis involved research, modeling, and experimentation for the solar collection system of the cooker. This thesis looked at prior research on glazing, Fresnel lenses, and absorber surface treatments to identify and evaluate elements for use in the collection system. Borosilicate glass, with a thermal conductivity of 1.005 W/mK and a solar transmittance of 0.91, and flat black paint, with absorptivity 0.96 and emissivity 0.88 were identified as potential elements for use in first trials.

Experimentation was performed on copper and aluminum samples with various surface treatments powered by various Fresnel lenses to evaluate the relative efficiency of these treatments. A novel treatment method, machining a conical hole into the sample, was found to improve efficiency on untreated samples, but inferior to flat black paint.

Modeling predicted that the minimum collection area for an acrylic Fresnel lens of f-number 1.2 was 0.60 m² for and 0.65 m² for the proposed collector without and with glazing, respectively. A recommendation of collection area 1 m² was proposed to account for unexpected losses due to manufacturing errors, positioning errors, and environmental variation.

This thesis also analyzed a proposal for a novel solar collector, a polished aluminum cone. Modeling and efficiency testing showed the cone to be inadequate for the radiation collection needed for the solar cooker.

Thesis Supervisor: David Gordon Wilson

Title: Professor Emeritus of Mechanical Engineering

1. Introduction

The work for this thesis consisted of modeling and testing the efficiency of different collection systems for use in a novel solar cooker under development by Professor David Gordon Wilson. The Wilson solar cooker is a cooker intended to store solar heat in a sealed container of lithium nitrate for six to seven hours during a tropical day. This should allow for storage of 5.4 megajoules of energy storage.

The solar cooker is being developed in response to several needs in the developing world. The consumption of biomass for cooking fuel leads both to pollution and desertification in the developing world. Additionally, the search for firewood may force women in dry tropical areas to walk ten to thirty km per day in search of firewood. Not only is this journey a hardship, but this search exposes them to rape and other forms of violence.

Solar cookers introduced into the developing world are often abandoned. Professor Wilson worked with VITA in northern Nigeria for two years and observed that many potential solar cooker users had a strong antipathy to both cooking and eating in the middle of very hot days. Thus, the solar cooker was left unused. The Wilson solar cooker is proposed to solve this problem by allowing thermal energy storage throughout the day via lithium nitrate.

The collection system for the cooker would be composed of a collector, absorber, salt, and insulation. This thesis tests to gauge the efficiency of the collector-absorber subsystems. Two collectors, an aluminum cone and a Fresnel lens, were considered for the system. For the absorber, aluminum and copper samples were tested. Some of these samples were untreated, while others were painted flat black to improve performance. Other samples had a conical hole machined into the receiving face to increase efficiency.

Development of a timing mechanism, cooker frame, and thermal modeling of the lithium nitrate and absorber are being performed in parallel by other project collaborators.

2. Background

2.1 Concentrating Collectors

A solar collector's efficiency, η , is defined as:

$$\eta_{collector} = \frac{\text{Useful power delivered by the collector}}{\text{Insolation falling on the collector}}$$

Where,

$$\begin{aligned} \text{Useful power delivered by the collector} \\ = \text{Power absorbed by system} - \text{Rate of heat loss to the environment} \end{aligned}$$

Heat loss occurs via conduction, convection, and radiation.

For processes like cooking that require high temperatures on the range of 120 to 250 °C, solar collectors often incorporate concentrators that focus solar radiation from a large collecting area S_1 onto a small target (absorber) area S_2 . The performance of such a concentrator is often characterized by the geometric concentration ratio, C , and the optical efficiency, $\eta_{concentrator}$. The optical efficiency is the radiative energy received at S_2 , Φ_2 , divided by the radiative energy passing through S_1 , Φ_1 .

A total measure of performance can be seen by optical concentration ratio or optical effectivity.

$$\eta_{concentrator} = (\Phi_2/S_2)/(\Phi_1/S_1)$$

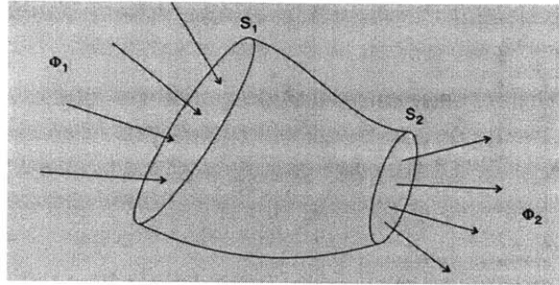


Figure 1: Concentrator diagram taken from reference 1.

The power absorbed by the system is expected to equal

$$\text{Power Absorbed by System} = \text{Insolation} * \eta_{concentrator} * \alpha$$

, where α is the absorptivity of the absorber.

The final absorber and thermal storage systems were not ready for testing as this thesis was being written. Thus, the power absorbed by the lithium nitrate, which would have been the best way to measure the power absorbed by the system was not available for testing. Thus, useful power delivered in this study is viewed as the power delivered in heating a copper or aluminum test sample. The useful power delivered can be calculated by the equation

$$\text{Useful Power Delivered} = m * c_p * \frac{\Delta T}{\Delta s}$$

, where c_p is the specific heat of the sample, m is the mass of the sample, and $\frac{\Delta T}{\Delta s}$ is the temperature rate of change. The specific heat of aluminum is 900 Joules/(Kilogram*Kelvin).² The specific heat of copper is 386 Joules/(Kilogram*Kelvin).²

2.2 Solar Insolation

The solar cooker relies on solar radiation from the sun to provide power. Solar radiation is mainly in the visible light spectrum and near infrared spectrum as shown in table 1 and figure 2. Because the sun is very far from the Earth, the radiation inflected on the earth at the top of the atmosphere is almost completely parallel with an average magnitude of 1.37 KW/m².³ A significant amount of this radiation is absorbed or scattered by clouds and air molecules, as shown in figure 2. On a very clear day this diffuse component accounts for 10 to 20% of the total solar radiation.⁴

The solar insolation on a clear day during daytime over a wide area of the tropics between latitudes of +/- 15 degrees can be taken as about 1 KW/m².⁵ On clear days in Boston, the author's pyranometer typically read 1200 W/m². It is possible that some of this radiation was diffuse radiation.

| Wavelength (μm) | Fraction of Total | Energy Flux for Fraction |
|---------------------------------------|-------------------|--|
| 0.00 - 0.38 (gamma to ultraviolet) | 0.0700 | 95 W/m ² 30 Btu/hft ² |
| 0.38 - 0.78 (visible) | 0.4729 | 640 W/m ² 203 Btu/hft ² |
| 0.78 - 2.0 (near infrared) | 0.3920 | 530 W/m ² 168 Btu/hft ² |
| 2.0 - ∞ (infrared to radio) | 0.0651 | 88 W/m ² 28 Btu/hft ² |

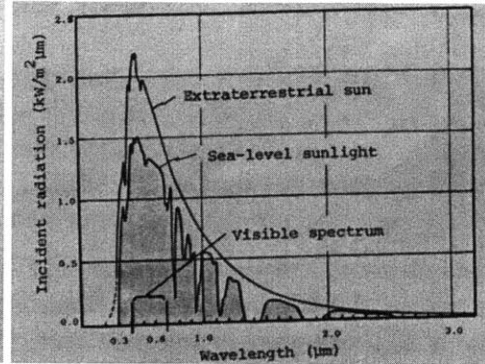


Table 1 (left): Wavelength distribution of radiation from the sun (top of atmosphere). Taken from reference 4.

Figure 2 (right): Graph of incident radiation as a function of wavelength at the top of atmosphere and sea level. Taken from reference 4.

2.3 Concentrators

The two concentrators proposed for the Wilson solar cooker were a polished aluminum cone and a Fresnel lens.

2.3.1 Polished Aluminum Cone

A polished aluminum cone was proposed by Peter Nylund as a way of concentrating the light. It was thought that with the right angle, the light would reflect several times off the interior surface down to the outlet of the cone. An angle of 42.5 degrees was chosen. The dimensions of the cone are as follows:

Height = 34.37"

Exit Diameter = .5" diameter

Entrance Diameter = 32" diameter

Angle = 42.5 degrees

Thickness = .032"

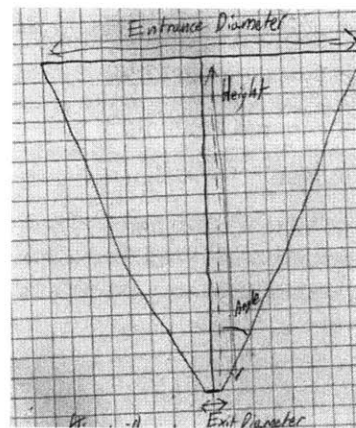


Figure 3: Sketch of cone with labeled dimensions.

A ray tracing analysis was performed for cone angles between 1 and 90 degrees. This analysis is based on the law of reflection that says light which hits a surface with a given angle of incidence will be reflected off the surface with the same angle of incidence. The angle of incidence of a ray to a surface is measured as the difference in angle between the ray and the normal vector of the surface at the point of intersection.

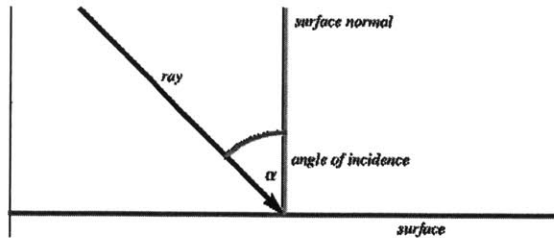


Figure 4: Diagram showing relation of angle of incidence to surface plane. Figure taken from reference 6.

For this analysis, the θ_{light} is the angle of light relative to the normal of the entrance plane. If light enters the cone with zero angle of incidence ($\theta_{\text{light}} = 0$) then the light will be reflected such that the light has a new θ_{light} which is twice the angle of the cone.

When light hits the next angle of the cone, it can then be shown that θ_{light} will increase by twice the angle of the cone. This pattern of reflection continues down the cone until the angle of light reaches the exit or is greater than 90° . At this point, the light is reflected out of the cone.

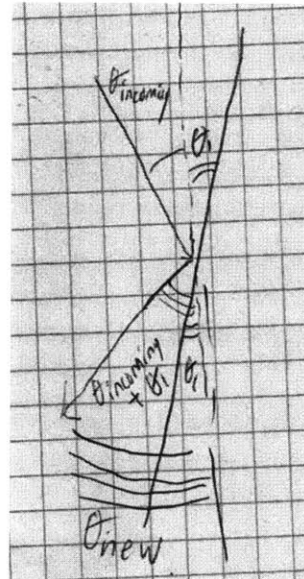
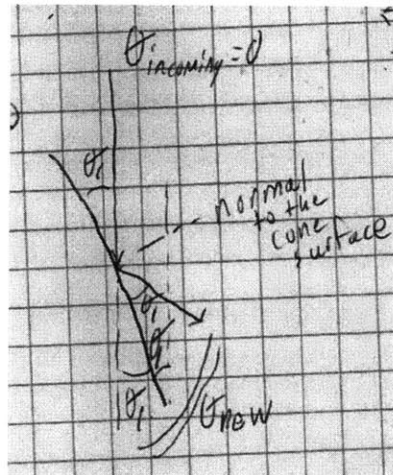


Figure 5: Path of light down an aluminum cone. $\theta_{\text{light}} = \theta_{\text{incoming}}$ before the reflection and $\theta_{\text{light}} = \theta_{\text{new}}$ after the reflection. (Left) First reflection of light. (Right) Second reflection of light.

Figure 6 shows the results of that analysis in terms of concentration ratios and expected power output assuming 100% reflection (no absorption or transmission) along the aluminum cone. Figure 6 also shows the max height and entrance width for which incoming rays parallel to the normal of entrance surface plane would reach the output of the cone. Rays at a height greater than the max height will be reflected out of the cone before reaching the exit. The entrance width is the diameter of the cone at the max height. These dimensions were found by backward ray tracing. As can be shown from the plots, a cone of any angle greater than 1° with base width less than 152.4 mm would have been incapable of providing the power needed for the cooker.

Ray tracing shows that for the dimensions of the tested cone, an angle of 42.5 degrees and exit diameter of 0.5 inch (12.7 mm), the light ray reflects once down the cone before being reflected out of the cone. The expected concentration ratio is 1.1658 and the expected power output is

0.5907 Watts. For the proposed cone, only rays 1.1 mm above the exit are expected to reach the exit.

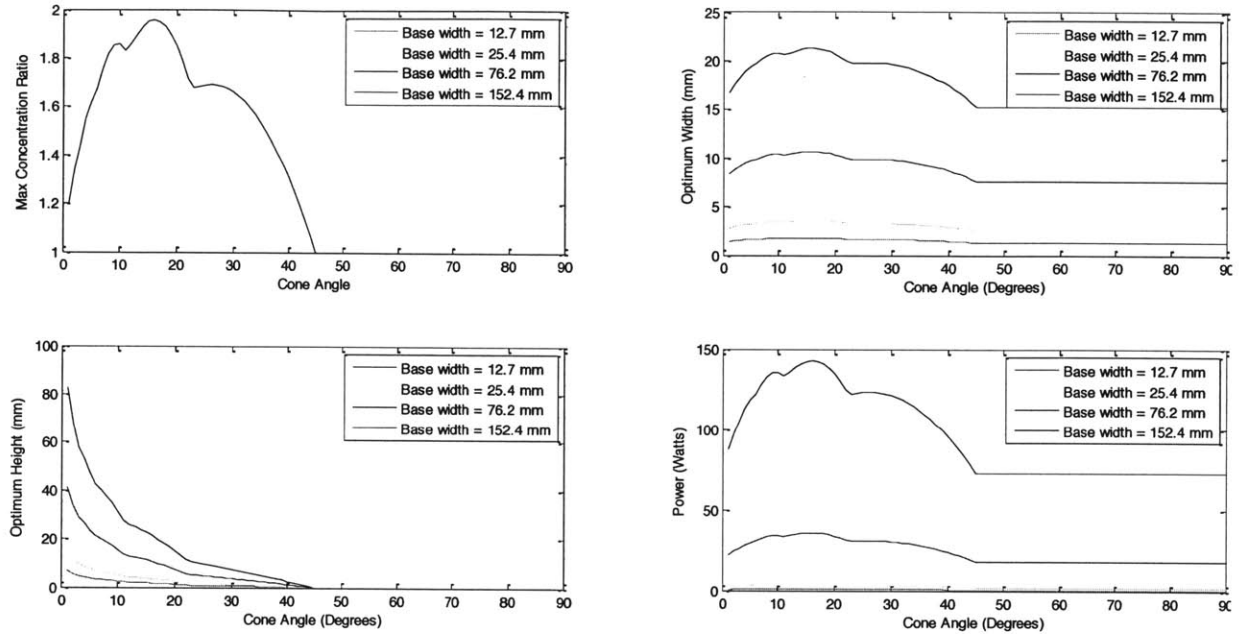


Figure 6: (From top left, clockwise) Plots of concentration ratio, optimum entrance diameter, optimum cone height, and expected power output for cone angles between 1 and 90 degrees. The curves represent different base diameters.

Figure 22 provides a picture of the aluminum cone used for testing.

2.3.2 Fresnel Lens

Fresnel lenses are special optical elements consisting of a thin piece of material into which concentric (spot Fresnel lens) or parallel (linear Fresnel lens) grooves are cut or molded. The Fresnel lens is an incredibly effective solar collector due to the fact that the grooves are shaped and arranged in such a way that each refracts light parallel to the optical axis at an angle necessary to make the majority of light passing through converge to a point or a line.

The transmittance of a solar collector is the primary measure of efficiency and describes the relationship between the solar irradiance incident on the cover and the irradiance that passes the cover on its way to the absorber. The transmission of a Fresnel lens, τ , is the product of the spectrally weighted reflected losses, τ_ρ , and the absorbed, τ_α , losses.

$$\tau = \tau_\rho * \tau_\alpha$$

Both the reflected losses and absorbed losses are influenced by a number of factors, including incident angle, manufacturing precision and accuracy, material properties, and the design of the lens itself.

Another defining characteristic of a Fresnel lens is its f-number (F #). This number is the ratio of the Fresnel lens focal length f , to the diameter of the lens.

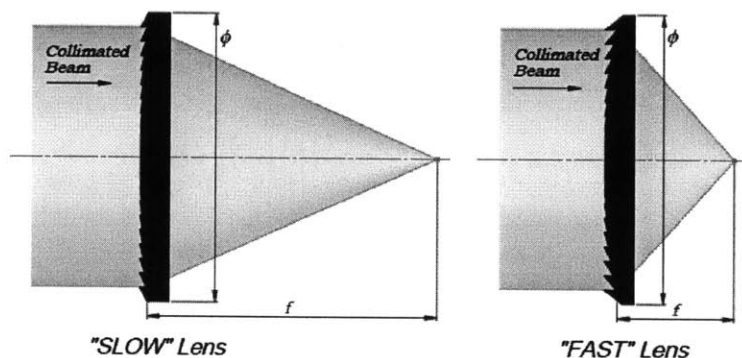


Figure 7: Demonstration of f-number. The lens focal length is f . The lens diameter is ϕ . The “fast” lens has a lower f-number than the “slow” lens. Caption and image taken from reference 7.

Fresnel lenses are almost universally plano-convex. For solar collection applications, the grooves on a Fresnel lens may be designed to be oriented towards the focus (absorber plate) or the collimated light source (sun). When the lens is designed for grooves oriented toward the collimated light source, or long conjugate, it is described as grooves “out”. When the lens is designed for orientation towards the focus, or short conjugate, it is described as grooves “in”.

There are performance tradeoffs for grooves in vs. grooves out lenses used for solar collection. Fresnel lenses are typically fabricated so that they are oriented correctly for grooves out. Best optical performance is achieved with this type of Fresnel lens, as both plane and convex surfaces refract the light more or less equally.

In the grooves in case, the grooves at the outer periphery of the lens are cut at much smaller angles to the plano surface than they would be in the grooves out case. Because the angles are relatively small toward the periphery of the lens, any small warpage or tilt of the lens surface or deviation of the light ray from parallelism with the optical axis leads to an enhanced deviation from the ideal in angle between the light ray and the lens surface. These errors lead to the primary decrease in the collection efficiency of a grooves “in” vs. an “out” lens of same focal length and f-number. However, grooves in lenses are often desirable, as the orientation minimizes dust build-up in the grooves steps. Photovoltaic applications typically use grooves in lenses.

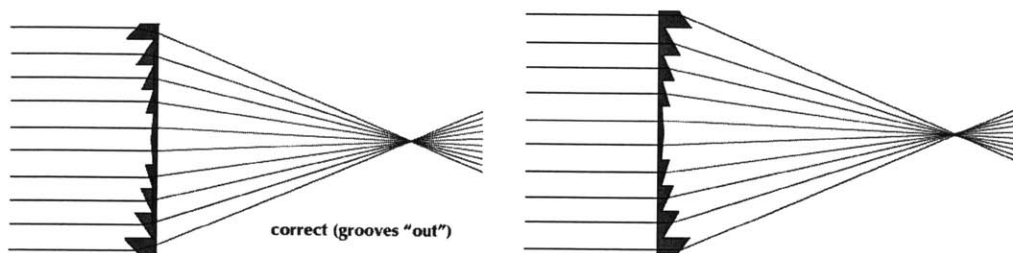


Figure 8: (left) Grooves “out” lens. (right) Grooves “in” lens. Taken from reference 8.

A comparison of optical efficiency for an Acrylic (Poly(methyl methacrylate) or PMMA) concentrating grooves “in” lens and grooves “out” lens is show in figure 9.

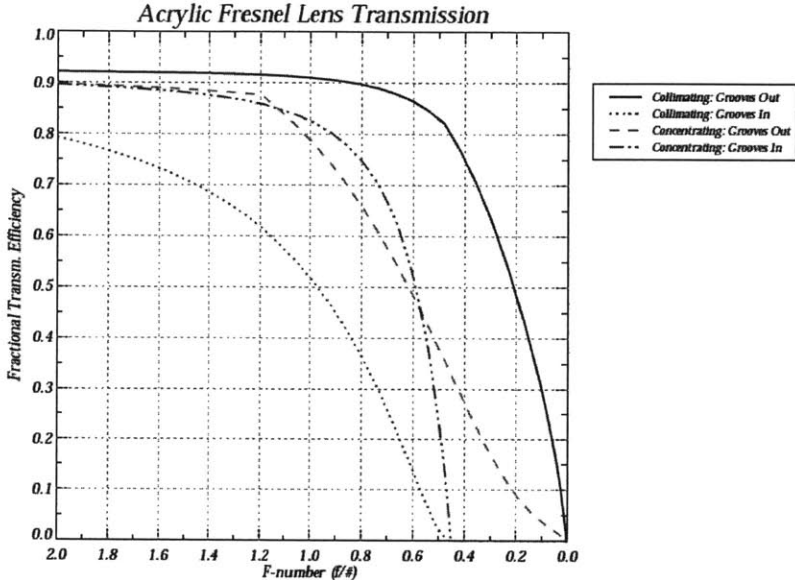


Figure 9: Idealized efficiency values for Acrylic (PMMA) Fresnel lens configurations based on modeling and simulations performed by Arthur Davis. Taken from reference 9.

Another key feature of a Fresnel lens is the groove geometry portrayed in figure 10. The grooves have a slope angle component (the component acting to refract the rays) and a draft component (which would optimally be 0 degrees for best optical performance). Incidence on the draft facet incurs losses, as the light going through the draft facet takes a trajectory that deviates from the focal point.

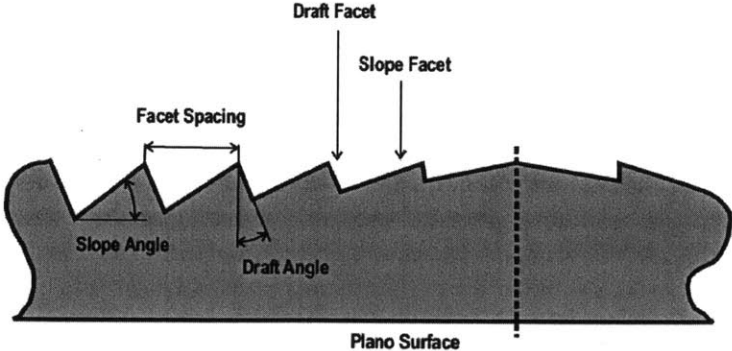
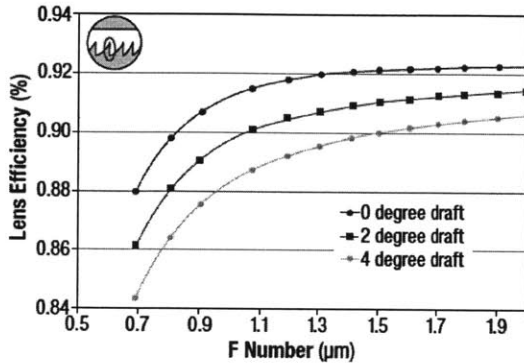


Figure 10: Side-profile schematic of Fresnel lens prisms. Taken from reference 7.

Deviations in groove geometry from the ideal harm the efficiency of the lens. Draft angles greater than zero and groove (prism) tip rounding are the main examples of losses due to manufacturing. Figure 11 is taken from shows the efficiency loss due to these deviations. A third manufacturing source of losses comes from the unavoidable width of the vertical step between the grooves.

Draft Angle

Losses due to the unused (draft) facet for several draft angles are illustrated in the following graph. The ideal case of 0° draft angle is difficult to meet in lens production.



Facet Corner Rounding

Facet corner rounding is an indication of replication fidelity. It is difficult in most molding processes to get high fidelity replication with the fast cycle times required to produce lenses at low cost.

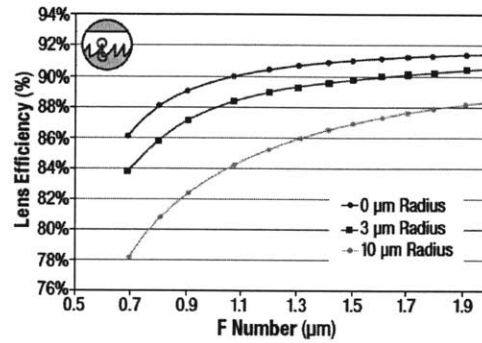


Figure 11: Approximation of losses due to variations in draft angle and prism tip rounding. Figure taken from Reference 10.

Fresnel lenses used for solar collection are typically made of acrylic, polycarbonate or rigid vinyl. Transmission plots for different wavelengths are provided in figures 12 below. Both the thickness of the material and the type of material effect the losses due to absorption.

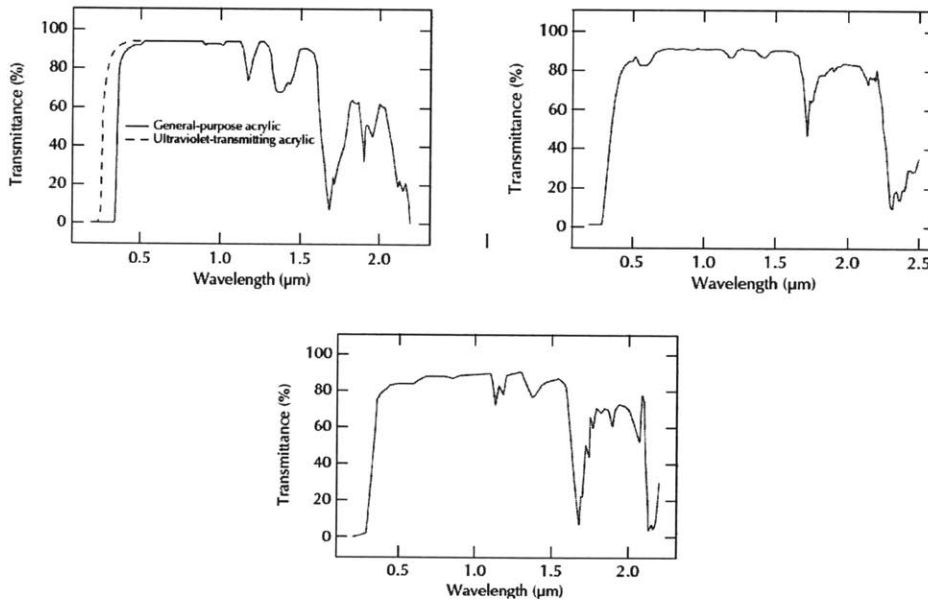


Figure 12: (top left) Transmittance of general purpose acrylic as a function of wavelength for sample thickness of 3.2 mm. (top right) transmittance of rigid vinyl as a function of wavelength for sample thickness of 0.76mm. (bottom) Transmittance of polycarbonate as a function of wavelength for sample thickness 3.2 mm. Figure taken from reference 8.

Reflection at the lens surface is another source of Fresnel lens collector losses. Some reflection is inherent in due to the material and geometric properties of the Fresnel lens. Additionally, the angle of incidence of incoming light is a source of reflective losses.

As the angle of incidence increases, so do reflection losses, as shown in figure 13. For the Fresnel tests, the angle of incidence was kept as close to zero as possible, to minimize these losses. Grooves “out” lens incur extra reflection losses with deviation in angle of incidence due to shadowing and blocking effects occur from the vertical step.

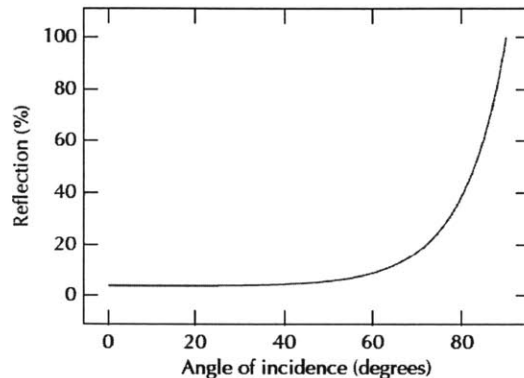


Figure 13: Percentage of light reflected as a function of angle of incidence with the plane of the Fresnel lens. Figure taken from reference 10.

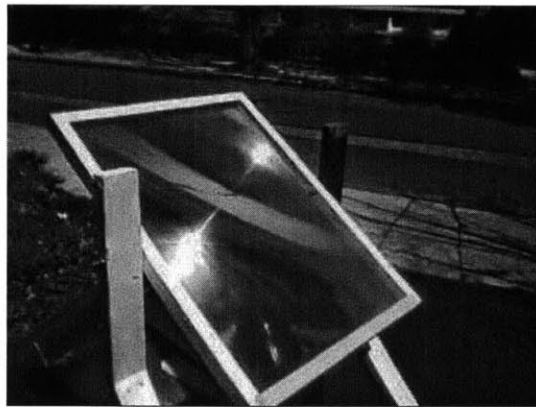


Figure 14: The figure clearly shows reflection on the face of a Fresnel lens with close to zero degree angle of incidence.

The Fresnel lenses used during testing were rectangular Fresnel lenses with surface areas of 0.86 m^2 and 0.505 m^2 and estimated f-numbers of 1.07 and 1.40 respectively. They were made of acrylic (PMMA), for which the transmittance across the solar spectrum is roughly 0.92.⁸ The larger Fresnel lens had some damage from burning.

2.2 Absorbers

Absorbers are elements used to collect the solar insolation and convert it into heat. Absorbers are defined by two properties: absorptivity, the % of radiation the absorber converts into energy over the solar spectrum, and emissivity a value that indicates how much radiation an absorber radiates to the environment at a given temperature. A good absorber has a high absorptivity and a

low emissivity to maximize the radiation it receives and minimize the radiation it gives off to the environment.

The Stefan-Boltzmann law states that a blackbody radiator will emit radiation according to the following equation,

$$P = e * \sigma * A * (T^4 - T_a^4)$$

, where P is the power output of the body, e is the emissivity of the body, σ is Stefan's constant ($\sigma = 5.6703 * \frac{10^{-8}W}{m^2 \cdot K^4}$), A is the surface area of the body, T is the temperature of the body, and T_a is the ambient temperature.

For the Wilson solar cooker, a copper plate was identified as the material of choice for the absorber plate. Both copper and aluminum were used during experimentation to evaluate the different type of absorber treatments. Aluminum was used due to its low cost.

Untreated copper and aluminum surfaces have low absorptivity, making them poor choices for the absorber. Various surface treatments were considered for the copper and aluminum. A chart of absorptivity and emissivity is given for the absorber surfaces considered. Selective absorber surfaces, such as surface treated with TiNOX®, Black CuO, Black Chrome, or Solchrome are surfaces treated to have high absorptivity and low emissivity. However, these treatments are usually relatively expensive. Figure 15 provides a model of absorber efficiency for these various surfaces under conditions similar to those expected for the Wilson Solar Cooker.

$$\text{Absorber Efficiency} = (\text{Radiation Absorbed} - \text{Radiation Emitted}) / \text{Insolation}$$

For this model, it is assumed that a collector collects all the radiation over a meter squared area and focuses it down to an area of 0.0232 meters², the size of the aluminum block used for testing. The solar insolation is assumed to be 1000W/m². The ambient temperature is assumed to be 15 degrees Celsius.

For this model, it seems that a copper plate coated with Solchrome would offer the best absorber performance. The modeling also shows a good performance for black paint, a cheaper alternative to a selective coating, especially at low temperatures. For testing, Rust-Oleum® flat black, high temperature paint was used.

Table 2: Absorptivity and Emissivity values for various absorber surface treatments. Values taken from references 11, 12, and 13.

| <u>Surface</u> | <u>Absorptivity</u> | <u>Emissivity</u> |
|---------------------|---------------------|-------------------|
| Buffed Aluminum | 0.16 | 0.03 |
| Buffed Copper | 0.30 | 0.03 |
| Black Paint | 0.96 | 0.88 |
| TiNOX® | 0.95 | 0.04 |
| Black CuO on Copper | 0.90 | 0.11 |
| Black Chrome | 0.93 | 0.10 |
| Solchrome | 0.96 | 0.12 |

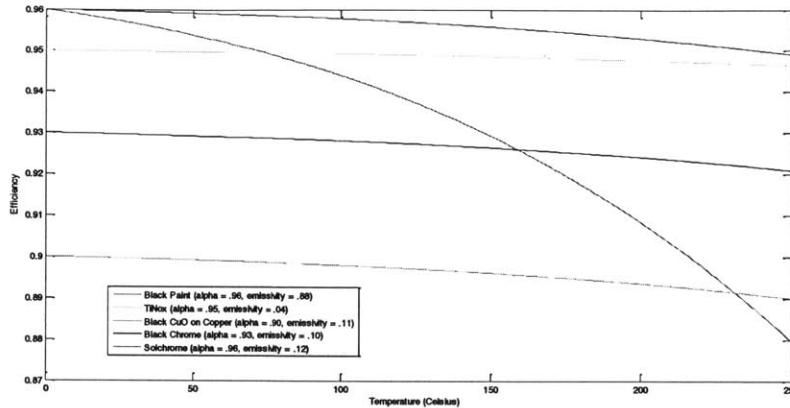


Figure 15: Efficiency vs. temperature of absorber modeled for various surface coatings on a plate with area 0.0232 meters²

It was also proposed that a machined conical hole on the surface of an absorber plate may improve efficiency by having light bounce around and be reflected inside the hole. A conical hole was machined into the centroid of the aluminum and copper surfaces with a stepless conical drill bit. The dimensions of the hole in the aluminum surface were as follows: a base diameter of 0.23”, a depth of 0.5”, and angle of 25 degrees. The dimensions of the hole in the copper surface were as follows: a base diameter of 0.34”, a depth of 0.75”, and angle of 25 degrees.

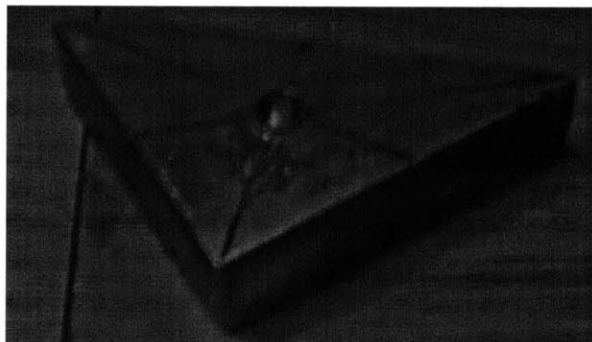


Figure 16: Conical hole machined into copper sample

2.4 Expected Efficiency and Total Losses

The solar collector systems proposed for the cooker suffer from several sources of loss. There are losses from the absorptivity of the absorber, the transmission of the collector, convection, and radiation into the environment. The previous sections have covered losses from the absorptivity of the absorber, the transmission of the collector, and radiation into the environment.

2.4.1 Convection Losses

A model to estimate the losses due to convection for the collector system is proposed by Kumar and Mullick.¹⁴ They reviewed several past attempts at approximating a convective heat

transfer coefficient for outdoor flat plate collectors conditions subject to wind. They point to McAdams who propose a heat transfer coefficient, h_w , as a function of the wind speed, V_w :

$$h_w = 5.7 + 3.8V_w$$

For V_w less than or equal to 5 m/s. This coefficient allows modeling of the convection losses to the collector system. The convection equation for the collector plate:

$$\dot{Q} = h_w * A * \frac{\Delta T}{\Delta s}$$

Where \dot{Q} is the rate of heat transfer from the collector plate, A is the surface area of the collector plate.

2.4.2 Glazing

A transparent cover plate (glazing) can be placed on an absorber surface to improve the efficiency by reducing the rate of heat loss, both convective and radiative, from the surface. 98% of energy in incoming solar radiation is contained within wavelengths below 3 micrometers, whereas 99 per cent of radiation emitted by black or gray surfaces at 400K is at wavelengths longer than 3 micrometers. Ideal glazing materials transmit the majority of sunlight but does not transmit the high wavelength radiation emitted by a black body. Additionally, ideal glazing has a low thermal conductivity to reduce convective heat transfer from the absorber surface.

A low thermal conductivity, k , reduces the overall heat transfer coefficient, U , where,

$$U = 1/((1/h_w) + (\Delta x/k))$$

The influence of the overall heat transfer coefficient on the conductive/convective heat transfer of the plate is described below:

Thicker glazing (larger Δx) reduces the heat transfer to the outside environment but also increases transmittance losses due to reflection and absorption. Glass and various plastics are typical glazing material.

Plastics tend to be cheaper and sturdier than glass. They also tend to have lower thermal conductivity values. However, they tend to weaken or melt at high temperatures and can yellow and degrade under sunlight over time. The temperature limits of many plastics, such as acrylic, polycarbonate, and polyethylene, make them unsuitable for the intended application despite having excellent transmission and conductivity values. High temperature Teflon and fiberglass have been identified as plastics that may be able to meet the temperature requirements of the cooker. Teflon (thickness 0.25 mm) has a solar transmittance of 0.94 and a thermal conductivity of 0.25 W/(m*K).^{15,16}

Glass has a solar transmittance of roughly 0.91 and is opaque to most infrared radiation.¹⁷ 1/8 inch (3.175 mm) thick Heat-Resistant Borosilicate Glass was purchased for use in the collection system. The low conductivity, 1.005 W/(m*K) of glass also serves to reduce the convective heat transfer from the absorber surface.¹⁶

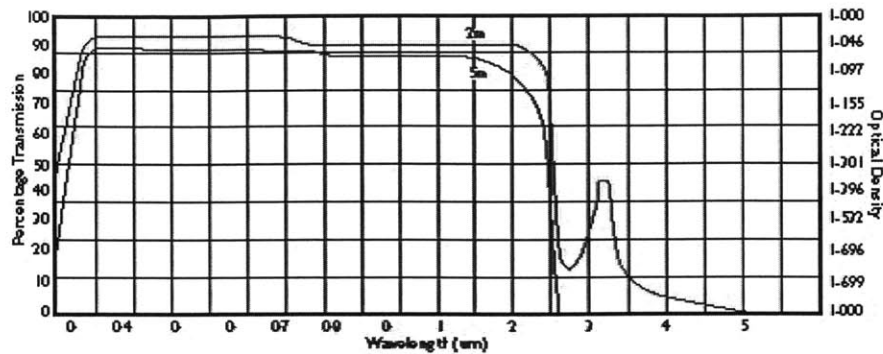


Figure 17: Transmission as a function of wavelength for Pyrex Borosilicate Glass. Figure taken from reference 17.

2.4.3 Modeling of the Test System

Three of the tests performed were modeled for efficiency assuming the following parameters and using the equations presented in the previous text. The results are shown in figure 18. The model was based off of a Fresnel lens with grooves out, as this was the configuration of the lens for the tests. Models were made for the aluminum with black paint for the large lens (0.860 m² area), the aluminum with black paint for the small lens (0.505 m² area), and the aluminum with black paint and glass glazing for the small lens.

$$V_w = 5 \text{ m/s}$$

$$\text{Insolation} = 1000 \text{ W/m}^2$$

$$\text{Ambient Temperature} = 15 \text{ degrees Celsius}$$

$$\text{Receiver Surface Area (A}_1\text{)} = 0.0232 \text{ m}^2$$

$$\text{Exposed Surface Area (A}_1\text{)} = 0.0464 \text{ m}^2$$

$$\text{F-number (Large lens)} = 1.07$$

$$\text{F-number (Small lens)} = 1.40$$

$$\text{Transmittance (Large Lens)} = 0.84$$

$$\text{Transmittance (Small Lens)} = 0.89$$

The transmittance of the Fresnel lens was estimated from the plot of idealized acrylic Fresnel efficiency as a function of f-number given in figure 9. The glazing is assumed to reduce the losses from emissivity on the glazed face to zero.

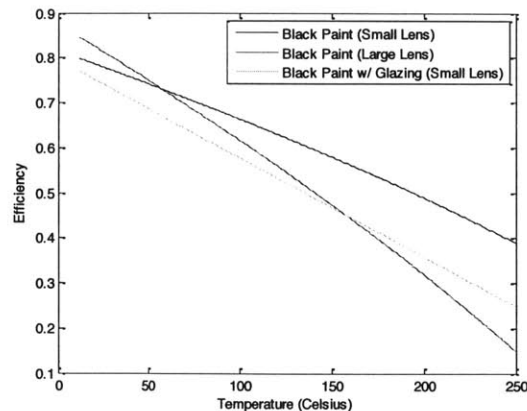


Figure 18: Modeled efficiency vs. temperature of experiment aluminum absorber plate. The different curves represent different surface treatments.

The tests kept the temperature of the sample between 0°C and 100°C. Thus, the expected efficiency range for aluminum samples with black paint (small lens) would be between 0.63 and 0.85, for samples with black paint (large lens) between 0.66 and 0.80, and for samples with glazing between 0.58 and 0.78.

2.4.4 Modeling of Power Absorbed for Proposed Cooker Collection System

The solar collector system currently proposed for the cooker is expected to be buffered from the wind and be rigorously insulated except for a ¼ inch diameter treated spot that will accept the incoming radiation from a Fresnel lens. Glazing has been considered for the system to prevent scratching and dust accumulation on the treated spot.

An important specification for this system is the useful power that will be delivered. It is desired that 500 Watts be delivered to the system at 250°C.

While this thesis doesn't provide an estimate of the losses due to heat transfer by the entire system (that modeling is being performed by other collaborators), it can provide an estimate of the power absorbed by the system to help the designer estimate this number. This analysis relies solely on losses due to transmission through the lens and glazing. This analysis also ignores losses due to manufacturing, wear & tear, or deviations from the angle of incidence. Thus the ideal power absorbed is

$$Power\ Absorbed = Insolation * A_{lens} * \tau * \tau_{glazing} * \alpha$$

Where, $\tau_{glazing}$, is the transmission of the glazing (.91 for glass). $\tau_{glazing}$ equals 1 if no glazing is present. The ideal power absorbed is temperature independent.

Plots of power absorbed vs. lens area were developed for both the system considered with and without glazing and shown in figure 19. An acrylic (PMMA) lens with f-number of 1.2 was assumed, giving an ideal transmission of 0.88. Insolation was assumed to be 1000 W/m². α was assumed to be .95, which is the absorptivity of flat black paint and close to the absorptivity of other selective surfaces.

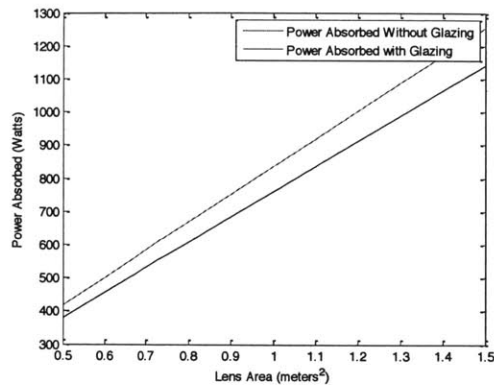


Figure 19: Plot of ideal power absorbed as a function of lens surface area for a cooker with and without glazing

From figure 19, the minimum ideal lens size to meet 500 Watts at 250°C is 0.60 m² for the system without glass glazing and 0.65m² for the system with glass glazing.

3. Experimental Design

Several collectors and absorber pairs were tested for their collection efficiency. For a given test, an absorber sample was heated with radiation from the collector for a period of 60 to 90 seconds. The first 10-15 seconds of each test were ignored to account for positioning time. Starting temperatures for the absorber sample varied between ambient temperature (0 degrees Celsius on some days) and 90 degrees. Samples were not heated above 100 degrees Celsius.

The tests were performed in clear skies in Boston, Massachusetts at various times throughout April and May 2014. During the tests, the solar insolation was measured at the beginning and end of the test with a SM206 Digital Solar Power Meter pyranometer. The resolution of the pyranometer was 0.1W/mm² or +/- 10 W/mm² or +/- 5% of the measured value.¹⁸ The average of the two measurements was used to approximate the insolation received by the collector. If the cloud cover changed was observed to change during the test, the test was discarded.

A Vernier k-type digital thermocouple was used to measure the temperature during the test. This thermocouple was able to tolerate temperatures between -200°C and 1400°C.¹⁹ The resolution was 0.2° Celsius.¹⁹ The data was recorded with a Lab Quest sensor interface using a data collection rate of 2 samples per second. This thermocouple was attached to the absorber sample with 3M VHB tape.

Support systems were developed for the Fresnel lens and polished aluminum cone. The lens came with a wooden frame. A ¼ in hole was manufactured at the midpoint of the frame and a bolt was put through the hole. The frame was held up by wooden posts as shown below. A nut and washer were placed on the bolt and tightened to the frame to hold the lens in place through friction.



Figure 20: (Left) Testing an aluminum sample with black paint. (Right) Fresnel lens frame and support.

The cone was held up by a support system built from PVC and wood. The support system is shown below. A PVC carriage was built to hold the aluminum cone and allow for easily manipulation. The PVC carriage was held up by wooden supports. A rope was tied between the PVC carriage and wooden braces and was used to control the angle of the aluminum cone.

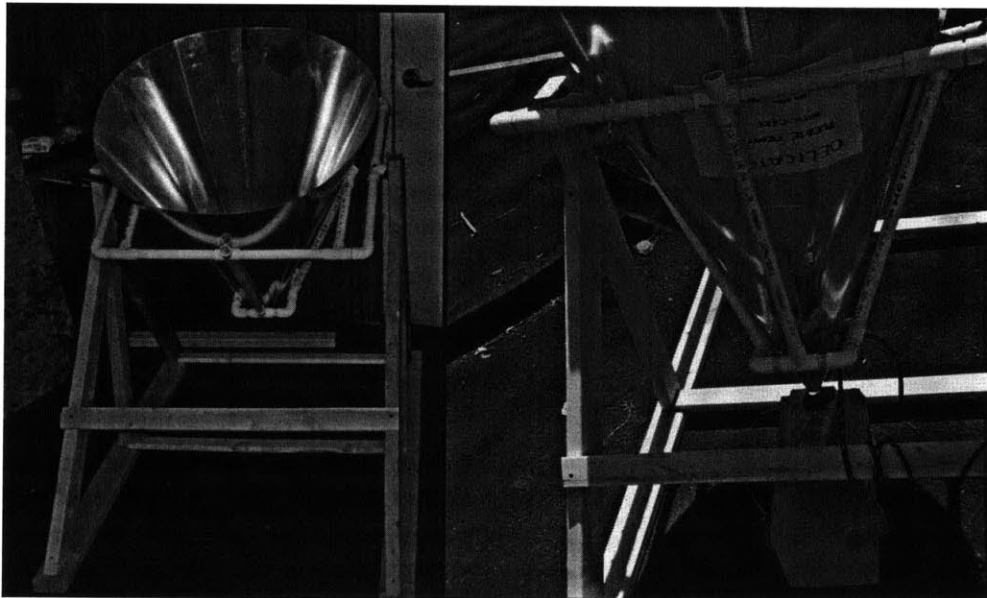


Figure 21 (left): PVC carriage and wooden frame for the aluminum cone. (right) Aluminum cone held in fixed position

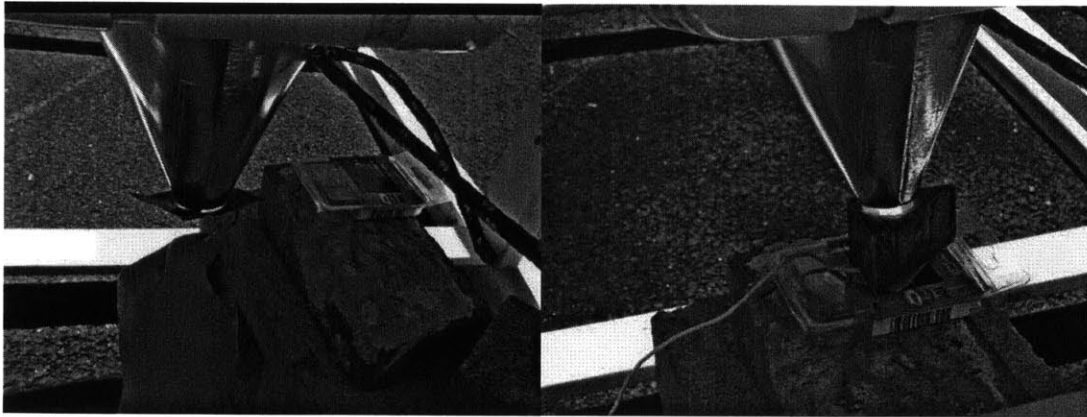


Figure 22: (left) Heating a sheet of aluminum painted flat black with the aluminum cone.
(right) Heating the copper block with flat black paint via the aluminum cone.

The sample rested either on cement and brick blocks adjusted to the focal point or was attached to a wooden plank and held at the focal point. A stand was developed to hold a given sample close to the focal point, although it was not used during testing.

The aluminum cone was tested with both a copper and aluminum sample painted with flat black paint. Additionally, the aluminum cone was tested with several sheet metal samples painted with flat black paint. Several Fresnel lenses with diameter of blank and blank were tested with copper or aluminum blocks with a receiving face with flat black paint, flat black paint and glazing, a machined conical hole, or unaltered.

3.1 Safety Considerations

Fresnel lens are dangerous and can cause fire, burns, and damage to vision. During testing, the experimenter took a number of precautions to avoid injury to himself and others. Neither the experimenter nor any other person were ever behind the lens when it was aimed towards the sun. Additionally, the experimenter wore welding goggles and kept the temperature of the samples relatively low so that they could be handled.

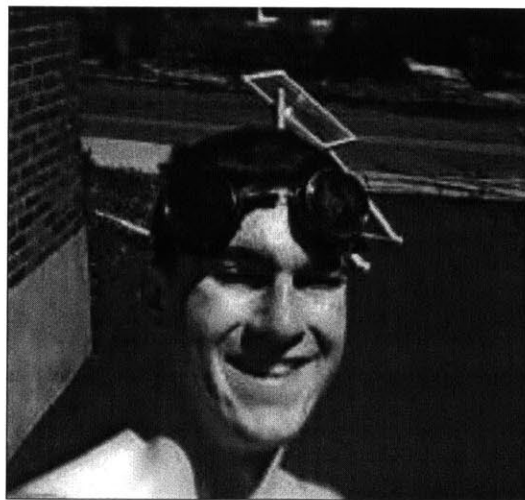


Figure 23: The author with welding goggles for safety.

4. Results and Discussion

The data for each test was post processed in logger pro and excel to assess the power absorbed, temperature rate of change, and efficiency for each test.

The testing of the aluminum cone proved it to be an ineffective solar concentrator. Five of six tests showed no clear increase in temperature. This was unsurprising given the ray tracing predictions given in Section 2.2. The sixth test gave the collector efficiency as 1.88%. This deviation is surprising, and may be due to fluctuations in ambient temperature during testing. During the testing, the temperature of the cone itself increased, showing that it clearly absorbed some of the incoming radiation.

Testing of multiple absorbers on several Fresnel lenses gave much more interesting results. These are presented in table x below.

Table 3: Table of testing data for various materials, surface treatments, and lens size

| Material | Treatment | Lens Area (m ²) | Average Efficiency | Standard Deviation | # of Trials |
|----------|---------------------|-----------------------------|--------------------|--------------------|-------------|
| Copper | Black Paint | 0.860 | 32.5 | 7.3 | 9 |
| Aluminum | Black Paint | 0.860 | 23.7 | 2.5 | 5 |
| Copper | Black Paint | 0.505 | 34.8 | 8.1 | 6 |
| Aluminum | Black Paint | 0.505 | 35.2 | 7.9 | 23 |
| Copper | Conical Hole | 0.505 | 22.7 | 6.5 | 7 |
| Aluminum | Conical Hole | 0.505 | 30.6 | 2.1 | 7 |
| Aluminum | None | 0.505 | 14.8 | 2.4 | 7 |
| Copper | None | 0.505 | 18.2 | 2.2 | 7 |
| Aluminum | Black Paint+Glazing | 0.505 | 44.6 | 4.5 | 8 |

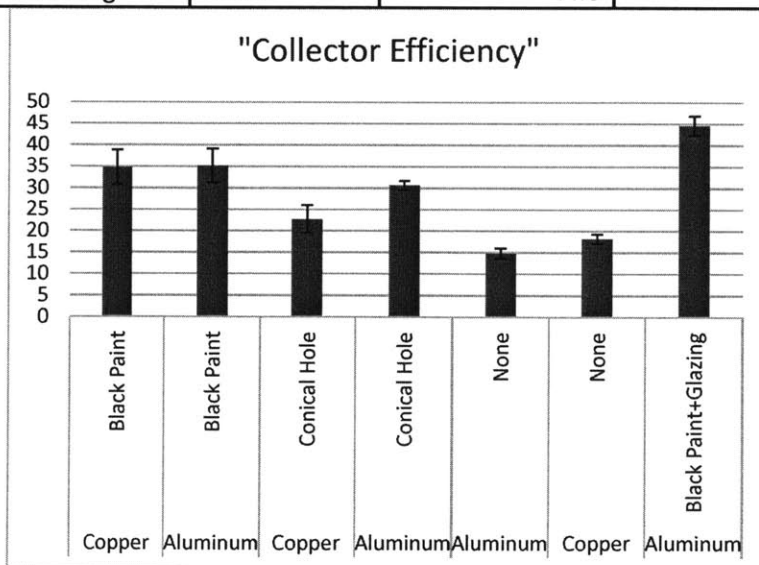


Figure 24: Comparison of collection efficiency for different absorber surface treatments powered by the 0.505 m² lens.

A number of interesting observations can be made from these results. First, it should be noted that the 0.86 m² (large) lens was 2.3 % less efficient for copper samples and 11.5% less efficient for aluminum samples than the 0.505 m² (small) lens. The difference in efficiency of the aluminum and copper samples for the larger lens is hard to explain. More trials are recommended to see if this difference holds true or was due to abnormal deviations in testing conditions (ex. abnormally high wind conditions). The overall difference in efficiency between the larger and smaller lens could be bolstered by damage on the large Fresnel lens that was caused by a fire during previous use.

The second observation is on the relative performance of the different surface treatments. Unsurprisingly, untreated aluminum and copper surfaces had the lowest efficiency of the methods tested. The conical hole showed an improvement in efficiency, but this improvement was not as great as the improvement due to the samples painted black with and without glazing.

The difference in average efficiency for the copper and aluminum samples with a conical hole is difficult to account for. In fact, this difference goes against expectations since copper has a higher absorptivity than and comparable emissivity to aluminum. More trials are recommended to see if this relation stays true or if it was potentially caused by deviations in testing conditions.

The relative performance of the black paint with glazing is also surprising. The modeling done in section 2.3.4, shows that for temperatures between 0°C and 100°C the glazing should be inferior in performance to the black paint due to the transmission losses incurred by the glazing. This might be accounted for in two ways. First, since some of these losses are from absorption, so they may actually be playing a role in heating the absorber system. Secondly, it should be noted that the key role of glazing between 0°C and 100°C is not reducing emissivity. Instead it is to reduce the convective heat transfer. If the convective heat transfer coefficient was larger than expected, the glazing may play a greater role in improving performance.

The final comment on these results is that all of the aluminum samples are notably below the predicted efficiency for temperatures between 0°C and 100°C. At the lower end, the difference between average test efficiency and expected efficiency was 32% for the black paint sample (large lens), 28% for the black paint sample (small lens), and 13% for the black paint sample with glazing. These losses could come from several sources outlined previously in the document. First, they could come from manufacturing errors and errors due to deviations in the angle of incidence. Secondly, they could come from errors in the estimated convection heat transfer coefficient due to a higher wind velocity or simply a poor model choice.

5 Conclusions/Recommendations

The research, modeling, and experimental results of this thesis yield several recommendations for cooker design decisions.

1. Both modeling and testing ruled out the aluminum cone as a viable collection system for the solar cooker
2. Flat black paint was shown to be a viable absorber coating, both through modeling and experimentation.
3. The conical hole was shown to be less effective than flat black paint. Further testing is recommended to see if treating a surface with both a conical hole and a surface coating, like black paint, will have better absorber perform than just the coated surface.

4. The research provides useful glazing and absorber coating alternatives.
5. The research provides useful values for the transmission loss for the lens and glazing. These values are used in section 2.3.4 to estimate the ideal power absorbed by the system and show the minimum Fresnel lens area is 0.60 m^2 for the system without glass glazing and 0.65 m^2 for the system with glass glazing.
6. Both research and testing shows that the designer should be prepared for significant unexpected losses (up to 300 watts) due to tracking error, manufacturing error, and increased heat transfer due to environmental conditions. Thus, a robust system that significantly overshoots the ideal minimum power delivered is desired. A Fresnel lens with a meter squared area is recommended to provide this kind of robustness.

Acknowledgments

My thanks go to Professor David Gordon Wilson for his mentorship on this project. I also wish to thank his wife, for bringing one of the Fresnel lenses to MIT. Additional thanks go to fellow project collaborators Dan, Austin, Hazel, and Julia. Finally, my thanks goes to the many authors of the work in my references. Without their work, my work would not have been possible.

References

- ¹R Leutz, A. Suzuki, *Nonimaging Fresnel Lenses*, Springer-Verlag Berlin Heidelberg, Germany, 2001.
- ²O. Humlum, "Solar Activity", <http://www.climate4you.com/Sun.htm>.
- ³R. Nave, "Table of Specific Heats", Georgia State University. Accessed on 5/22/2014 from <http://hyperphysics.phy-astr.gsu.edu/hbase/tables/sphtt.html#c1>.
- ⁴Y. Howell, J. Bereny, *Engineer's Guide to Solar Energy*, Solar Energy Information Services, United States of America, 1979.
- ⁵D.G. Wilson, "Development and Optimization of a Thermal-Storage Solar Cooker", MIT.
- ⁶W. K., Macura, "Angle of Incidence" From *MathWorld—A Wolfram Web Resource*, created by Eric W. Weisstein. <http://mathworld.wolfram.com/AngleofIncidence.html>.
- ⁷A. Davis, F Kuhnlenz, "Optical Design using Fresnel Lens", Reflexite Optical Solutions Business. Accessed online at http://www.orafol.com/tl_files/EnergyUSA/papers/Optical-Design-Using-Fresnel-Lenses.pdf.
- ⁸Fresnel Technologies, Inc., "Fresnel Lenses", 2012. Accessed online at <http://www.fresneltech.com/pdf/FresnelLenses.pdf>
- ⁹A. Davis, "Fresnel lens concentrator derivations and simulations", Reflexite Energy Solutions, Society of Photo-Optical Instrumentation Engineers. Accessed online at http://artdavis.wdfiles.com/local--files/optics-papers/Fresnel-lens-solar-concentrator-derivations-and-simulations_rev4a.pdf.
- ¹⁰3M, "Factors Influencing the Optical Efficiency of Fresnel Lens Concentrators", 2009. Accessed online at <http://bs1.lapptannehill.com/suppliers/literature/3m/Factors.pdf>.
- ¹¹Almeco GmbH, "Solar Absorber Coatings" Accessed online at http://www.almeocosolar.com/Brochure/tinox_energy_new_en.pdf.
- ¹²N. Madhukeshwara, E.S. Prakash, "An investigation on the performance characteristics of solar flat plate collectors with different selective surface coatings", *International Journal of Energy and the Environment*, Volume 3, Issue 1, 2012, pp. 99-108. Accessed online at http://www.ijee.ieefoundation.org/vol3/issue1/IJEE_10_v3n1.pdf
- ¹³G.M. Choudhury, "Selective Surface for efficient Solar Thermal Conversion", *Bangladesh Renewable Energy Newsletter*, 2002. Accessed online at <http://web.archive.org/web/20110616122534/www.bcas.net/Publication/EnergyNewsletter/Document/2003-5.PDF>.
- ¹⁴S. Kumar, S.C. Mullick "Wind heat transfer coefficient in solar collectors in outdoor conditions", Elsevier Ltd, *Solar Energy* Volume 84, Issue 6, June 2010, Pages 956–963 available online at <http://www.sciencedirect.com/science/article/pii/S0038092X10001076>.
- ¹⁵G. Reysa, "DuPont Plastic Film Glazing", [builditsolar.com](http://www.builditsolar.com/References/Glazing/DuPontFilms.htm) Accessed online at <http://www.builditsolar.com/References/Glazing/DuPontFilms.htm>.
- ¹⁶Engineering Toolbox, "Thermal Conductivity of some common Materials and Gases". Accessed online at http://www.engineeringtoolbox.com/thermal-conductivity-d_429.html.
- ¹⁷UQG Ltd, "CORNING PYREX® 7740 BOROSILICATE." Accessed online at http://www.uqgoptics.com/materials_commercial_corning_pyrexBorosilicate.aspx.
- ¹⁸<http://www.histest.com/drmeter-sm206-digital-solar-power-meter.html>
- ¹⁹Vernier Software & Technology, "Thermocouple", 2012, accessed online at <http://www.vernier.com/files/manuals/tca-bta.pdf>.